IJPSR (2020), Volume 11, Issue 10 **(Research Article)**

INTERNATIONAL JOURNAL OF PHARMACEUTICAL SCIENCES AND RESEARCH

Received on 31 October 2019; received in revised form, 26 February 2020; accepted, 20 March 2020; published 01 October 2020

COMPARATIVE MODELLING AND DOCKING STUDIES OF CYTOCHROME C OXIDASE SUBUNIT 1 PROTEIN

Vaishnavi Mallojala [1], Keerthana Pasam [1], Shravan Kumar Gunda [* 2], Seshagiri Bandi [1, 2] and Mahmood Shaik [1, 2]

Department of Biotechnology [1], University College of Science, Saifabad, Osmania University, Hyderabad - 500007, Telangana, India.
Bioinformatics Division [2], PGRRCDE, Osmania University, Hyderabad - 500007, Telangana, India.

Keywords:

Cytochrome c oxidase, Homology modeling, Modeller9.21, Docking, Natural compounds

Correspondence to Author:
Shravan Kumar Gunda

Faculty,
Bioinformatics Division,
PGRRCDE, Osmania University,
Hyderabad - 500007, Telangana,
India.

E-mail: gunda14@gmail.com

ABSTRACT: Cytochrome c oxidase, a mitochondrial metalloenzyme acting as the terminal enzyme of the mitochondrial respiratory chain. It provides a critical function in cellular respiration in both eukaryotes and prokaryotes. The recent development in technology has enabled researchers to understand the genetic, molecular, structural, and functional properties of proteins to identify appropriate targets against diseases, and as a result, many anti-inflammatory and anti-proliferative drugs have been developed. In the absence of X-ray and NMR protein crystal structure, homology modeling provides a useful 3D model for a protein that is related to at least one known protein structure. In the present study, the 3D molecular structures of nine Cytochrome c oxidase subunit 1 protein from different species such as *Myxine glutinosa*, *Struthio camelus*, *Sus scrofa*, *Homo sapiens*, *Xenopus laevis*, *Halichoerus grypus*, *Zygogeomys trichopus*, *Buteo buteo*, and *Plasmodium falciparum* were predicted using homology modeling software MODDLLER. The modeled structures were docked using Autodock4.2 software with ten different natural compounds and three drugs as a control to study the molecular interactions of these compounds with the coat protein. The results show that all the compounds exhibited good interactions with modeled proteins.

INTRODUCTION: Cytochrome c oxidase (EC 1.9.3.1) is a complex metalloprotein. Cytochrome c oxidase provides a critical function in cellular respiration in both eukaryotes and prokaryotes [1]. The gene COI plays a central role in metabolism, and it is present in almost all eukaryotes [2]. Cytochrome c oxidase I as a standard for molecular barcoding of animals, was proposed by Hebert [3].

QUICK RESPONSE CODE

DOI: 10.13040/IJPSR.0975-8232.11(10).5148-57

This article can be accessed online on www.ijpsr.com

DOI link: http://dx.doi.org/10.13040/IJPSR.0975-8232.11(10).5148-57

Cox1 has a phylogenetic signal system than the other mitochondrial genes [4]. The enzyme Cytochrome *c* oxidase is a terminal enzyme of mitochondria and aerobic bacteria respiratory chains. It is crucial that the complexes of the respiratory chains are combined into the membranes of bacteria and mitochondria [5]. Cytochrome c oxidase is a transmembrane protein, it looks like Y shaped, and is located in the inner mitochondrial membrane [6].

Three subunits I, II, and III are mitochondrially encoded and are present in all eukaryotes. The enzyme catalyzes 4-electron reduction of O_2 to H_2O [7]. In eukaryotes, the enzyme Cytochrome c oxidase is encoded in two genomes.

These three subunits I, II, and III have been isolated and sequenced from fungus, yeast and mammalian sources [8] and for plants [9-12]. Hence, the aim of the present study is to build a three-dimensional structure of nine different important Cytochrome c oxidase subunit 1 protein from different species by using homology modeling.

In addition, this study also focuses on performing a molecular docking for the identification of the effective inhibitory activity of known broad-spectrum compounds using molecular docking studies.

MATERIALS AND METHODS: The amino acid sequences of the Cytochrome c oxidase (COX) proteins from different species *Myxine glutinosa* isolate (Uniprot ID: O21079), *Struthio camelus* (Uniport ID: O21399), *Sus scrofa* (Uniprot ID: O79876), *Homo sapiens* (Uniprot ID: P00395), *Xenopus laevis* (Uniprot ID: P00398), *Halichoerus grypus* (Uniprot ID: P38595), *Zygogeomys trichopus* (Uniprot ID: Q6EGH7), *Buteo buteo* (Uniprot ID: Q94WR7), *Plasmodium falciparum* (Uniprot ID: Q02766) were retrieved from the protein sequence database UniprotKB (www.uniprot.org).[13]

To find related protein templates in order to build models for these primary sequences, a sequence similarity search has been carried out separately by using Protein BLAST [14] tool against solved protein structures deposited in Protein Data Bank (PDB). ClustalX and ClustalW2 are used for the correction of alignment [15]. Modeller9.21 [16] was used to gain satisfactory models [17]. The modeller is an implementation of an automated approach to comparative modeling by satisfaction of spatial restraints, which employs position-dependent gap penalties based on structural information of the template for generating alignments [18].

After manually modifying the alignment input file in MODELLER 9.21 to match the template and query sequence, 20 models were generated and selected the PDB file on the basis of the Modeller Objective Function. The selected model was subjected to a series of tests for its internal consistency and reliability. Backbone conformation was evaluated by the inspection of the psi/phi Ramachandran plot obtained from PROCHECK analysis [19].

Active Site Prediction: The active site for docking was predicted using the Tripos Sybyl6.7 SiteID [20] module after adding hydrogen atoms to the modeled proteins. The amino acids fall under active site for all the modeled proteins are shown in **Table 2**. The potential binding sites were predicted and identified by the SiteID module by correlating and combining key criteria such as depth, exposure, temperature factor, hydrophobicity, solvent accessible surface, and hydrogen-bonding capability. While detecting the potential binding sites, the SiteID module generates necessary files required for performing Autodock4.2 docking studies.

Docking Studies: Molecular docking studies were performed to elucidate the binding mode of COX proteins and the ligands. A total of ten molecules were docked to the protein to locate the appropriate binding orientations and conformations of various inhibitors in the binding pocket using the Graphical User Interface program "Autodock4.2". [21] Auto Dock 4.2 is an automatic docking tool designed to predict how small molecules bind to a receptor of 3D structures, which generates grids and calculates the docking score to evaluate the conformers. Gasteiger - Huckel united atom charges, polar hydrogen's and solvation parameters were added to the receptor for the preparation of protein in docking simulation, Gasteiger - Huckel charges assigned and then non-polar hydrogens were merged as the docking ligands were not peptides. All torsions were allowed to rotate during docking. The generation of PDBQT files for protein and ligands preparation, grid box creation, was carried out with Auto Dock Tools 1.5.6 (ADT) [22]. AutoDock saved the prepared ligand file and the PDB file in PDBQT format. Generated AutoGrid was used for the preparation of the grid map using a grid box. The grid size was set to 60 × 60 × 60 XYZ points, and the grid center was designated at dimensions (x, y and z). In Autodock, both the protein and ligands are considered as rigid. The binding poses with the lowest docked energy belonging to the top-ranked cluster were selected as the final model for post-docking analysis.

RESULTS AND DISCUSSION:

Homology Modelling of Proteins: After protein BLAST of the primary sequences of COX proteins with the predetermined structures deposited in PDB

bank, sequences that showed the greatest similarity were considered as template sequences. Twenty models were generated using the MODELLER 9.21 program based on the sequence alignment files generated by the ClustalX program. The alignment file was tweaked manually to best fit the sequences. Among the generated models for all the primary sequences, the model with the least object function was selected for further evaluation for protein stereochemistry (phi and psi angles) with PROCHECK software. The final models were validated using PROCHECK. The PROCHECK software generates a number of files that list complete residue by residue data and the assessment of the overall quality of generated structure compared to well-refined structures of the same resolution.

Fig. 1 shows the predicted homology models of all the Cytochrome c oxidase subunit 1 proteins belonging to different species. The Ramachandran plots for all the generated models are shown in **Fig. 2**. **Table 1** shows the residues falling in different regions of the Ramachandran plot. The results show that there are no amino acids falling in the disallowed region of the plot and a minor percentage of amino acids in the generously allowed regions, which indicate that the models are the better conformational structures. The template protein showed 87.7% of amino acid residues in the most favored region, 11.3% of amino acid residues in the additionally allowed region, 0.6% of amino acids in the generously allowed region, and 0.4% of amino acids in the disallowed region. Loop building was performed by using SPDBV.

TABLE 1: % OF RESIDUES FALLING IN DIFFERENT REGIONS OF RAMACHANDRAN PLOT OF CYTOCHROME C OXIDASE SUBUNIT 1 PROTEINS FROM DIFFERENT SPECIES

S. no.	Name of species	Core region		Allowed region		Generously allowed region		Disallowed region	
		No. of residues	%	No. of residues	%	No. of residues	%	No. of residues	%
1	O21079 *Myxine glutinosa*	416	94.3	24	5.4	1	0.2	0	0
2	O21399 *Struthio camelus*	416	95.4	18	4.1	2	0.5	0	0
3	O79876 *Sus scrofa*	419	95.9	15	3.4	3	0.7	0	0
4	P00395 *Homo sapiens*	416	95.4	16	3.7	4	0.9	0	0
5	P00398 *Xenopus laevis*	414	93.0	28	6.3	3	0.7	0	0
6	P38595 *Halichoerus grypus*	409	93.6	24	5.5	4	0.9	0	0
7	Q6EGH7 *Zygogeomys trichopus*	416	95.0	19	4.3	4	0.7	0	0
8	Q94WR7 *Buteo buteo*	413	94.7	18	4.1	5	1.1	0	0
9	Q02766 *Plasmodium falciparum*	393	94.7	17	4.1	5	1.2	0	0

Docking Studies of Modeled Proteins: The active site for docking was predicted using the Tripos Sybyl 6.7 SiteID module, and the active site is shown in **Table 2**. During the docking procedure, selected only the best fit, active site pocket with respect to the ligands in order to dock them. AutoDock 4.2 was used for molecular docking studies. Results obtained from AutoDock 4.2 provided information on the binding orientation of ligand-receptor interactions. Free energies of binding (ΔGb) and dissociation constants (Ki) as calculated by AutoDock4.2. The modeled protein was docked with natural compounds consisting of Plant compounds like flavonoids, phenolic compounds, alkaloids, *etc*. The docking programs place both the ligand and protein molecule in various orientations, conformational positions, and the lowest energy confirmations, which are energetically favorable are evaluated and analyzed for interactions. All the ten molecules that were docked showed good interactions.

From the docking simulation, we observed the free energy charge of binding for the protein-ligand complex. A possible explanation may be that the radio-graphical structure of the protein from

crystals differs from that of the aqueous system. The total energy was calculated for all the compounds against different targets are summarized in **Table 3-11**. Therefore, it can be concluded that the interaction of all the compounds with the corresponding targets is hydrophobic interactions in nature. Molecular docking indicated that the distance of hydrogen bonding between the ligand and the protein, respectively.

Molecular interaction between Cycloartocarpin A with different targets calculated the docking score. The modeled protein was used for molecular docking analysis. It was found that Cycloartocarpin A made a hydrogen bond with Gly355 with binding energy of -10.27 kcal/mol a P00395-Homo sapiens Cytochrome c oxidase subunit 1 protein. The compound also showed best interactions with Trp127 and Arg439 with binding energy of -10.49 kcal/mol an O21399-*Struthio camelus* protein.

It also shows Hydrogen bond interaction with the amino acid residue Met178 of modeled protein (Uniprot ID: O21079-*Myxine glutinosa*), a COX target with a binding energy of -6.26 kcal/mol. Four proteins showed the highest binding energy, and interactions with Cycloartocarpin A and other proteins showed the highest binding energy and interactions with other proteins. Similarly, we docked with the following targets O79876_Sus scrofa, P00395-Homo sapiens, P00398-Xenopus laevis, P38595-Halichoerus grypus, Q6EGH7-*Zygogeomys trichopus*, Q94WR7-Buteo buteo, Q02766-Plasmodium falciparum. Total ten natural compounds were docked with all the nine modeled proteins, and the results of the highest binding energy conformations and interacting amino acids are shown in **Fig. 3**. All the natural compounds exhibited good binding energies and interactions than standard drugs.

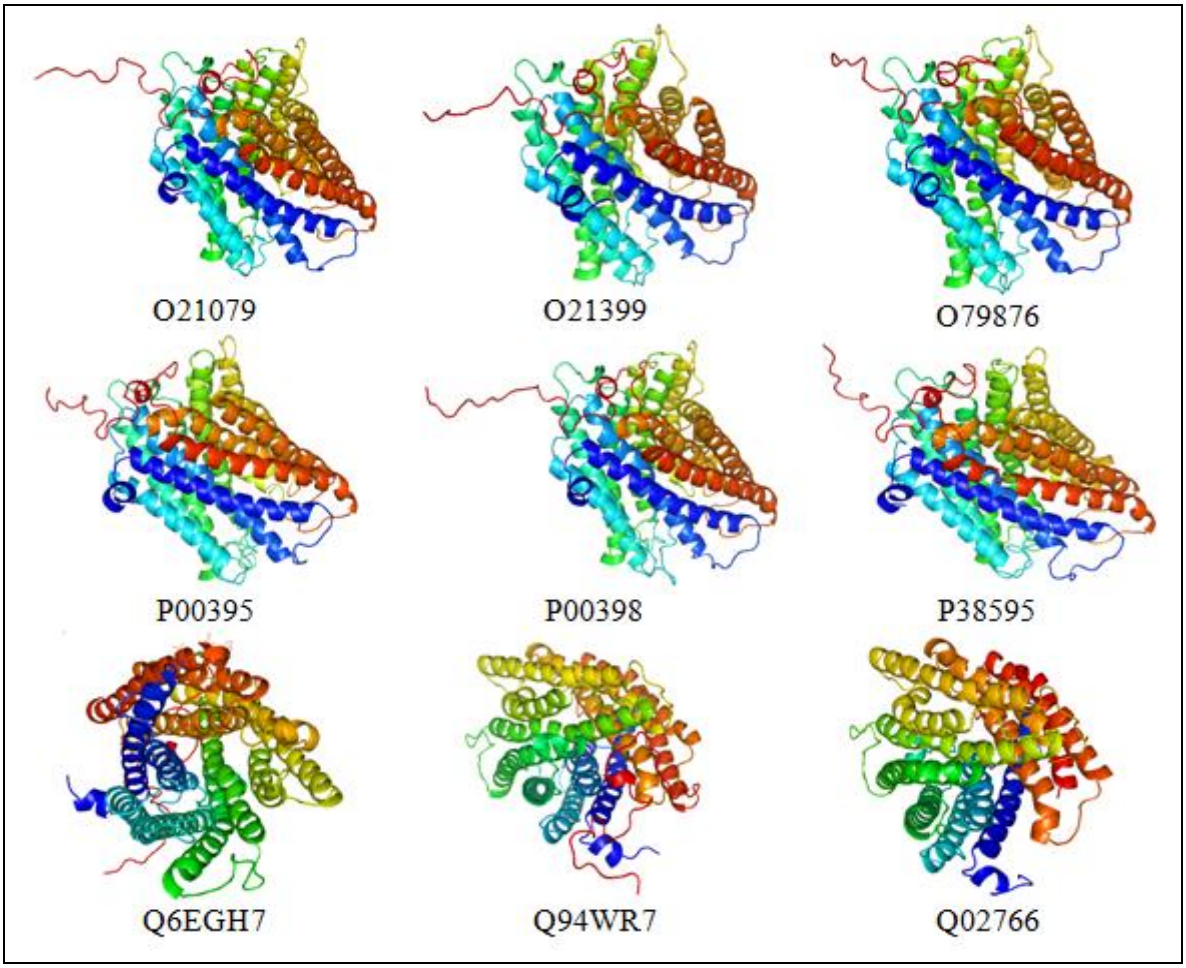

FIG. 1: HOMOLOGY MODELS OF CYTOCHROME C OXIDASE SUBUNIT 1 PROTEINS [A] *MYXINE GLUTINOSA* (UNIPROT ID: O2179), [B]*STRUTHIO CAMELUS* (UNIPORT ID: O21399), [C] *SUS SCROFA* (UNIPROT ID: O79876), [D] *HOMO SAPIENS* (UNIPROT ID: P00395), [E] *XENOPUS LAEVIS* (UNIPROT ID: P00398), [F] *HALICHOERUS GRYPUS* (UNIPROT ID: P38595), [G]*ZYGOGEOMYS TRICHOPUS* (UNIPROT ID: Q6EGH7), [H]*BUTEO BUTEO*(UNIPROT ID: Q94WR7), *[I]PLASMODIUM FALCIPARUM*(UNIPROT ID: Q02766).

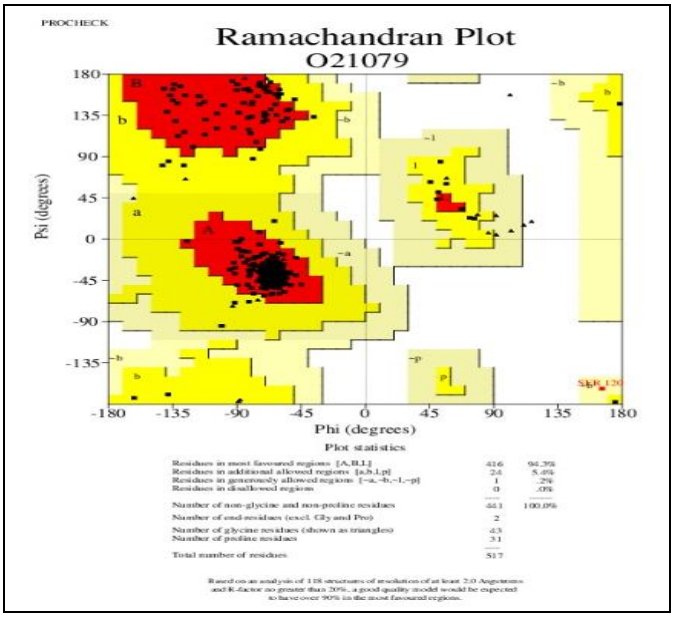
PROCHECK
Ramachandran Plot
O21079
Psi (degrees)
Phi (degrees)
Plot statistics

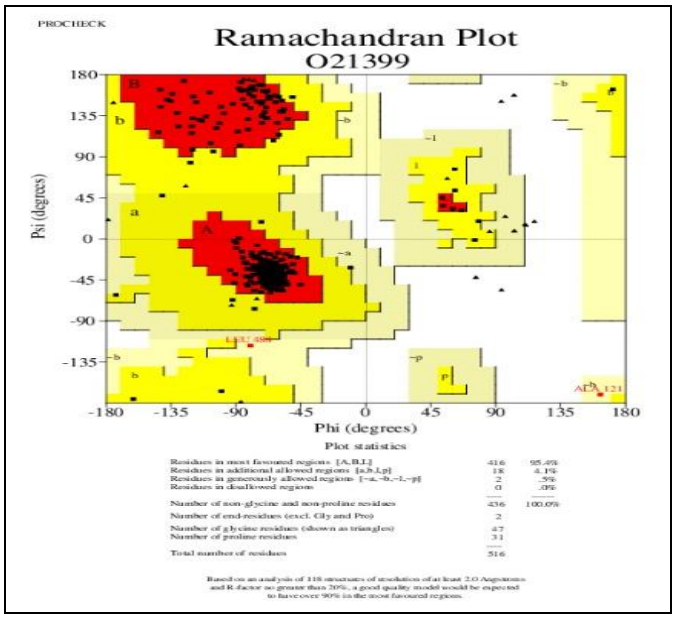
PROCHECK
Ramachandran Plot
O21399
Psi (degrees)
Phi (degrees)
Plot statistics

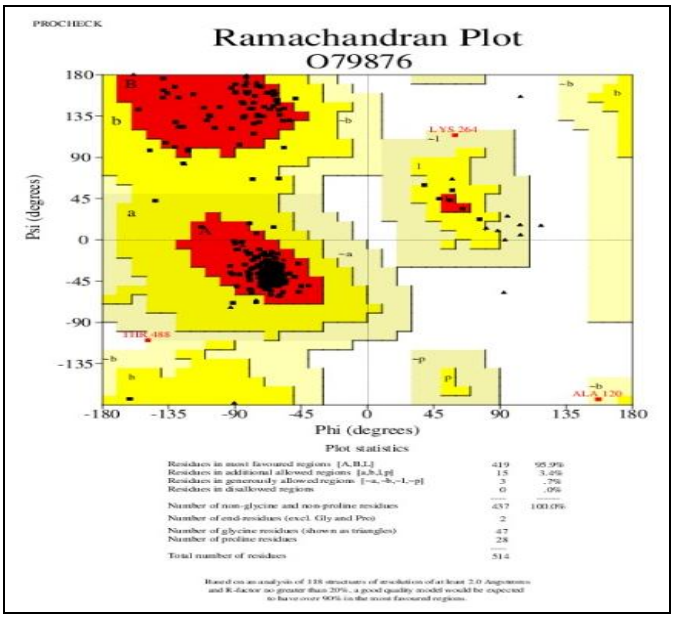
PROCHECK
Ramachandran Plot
O79876
Psi (degrees)
Phi (degrees)
Plot statistics

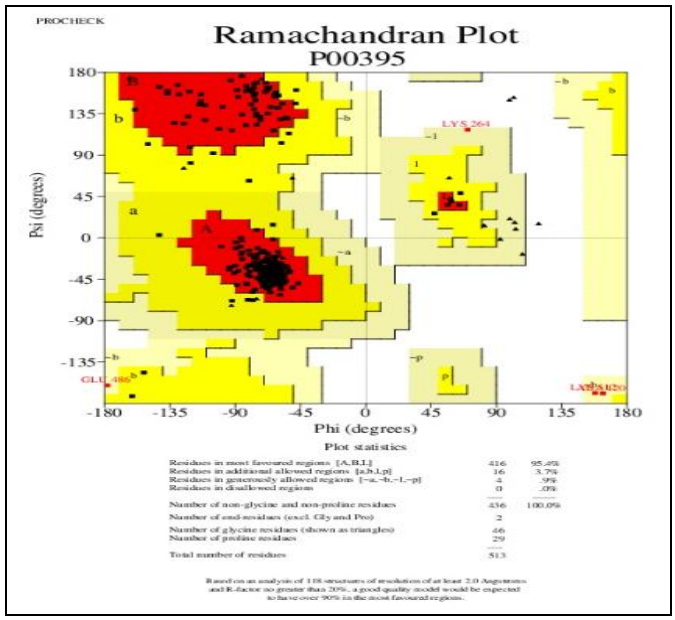
PROCHECK
Ramachandran Plot
P00395
Psi (degrees)
Phi (degrees)
Plot statistics

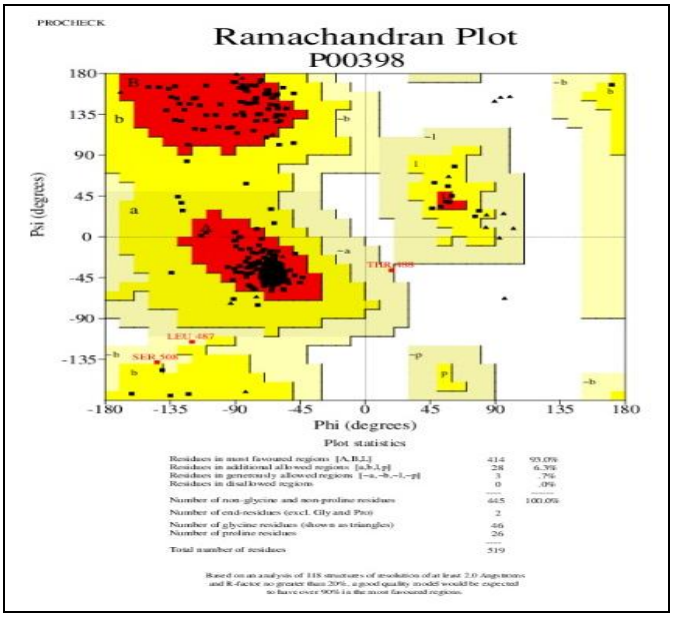
PROCHECK
Ramachandran Plot
P00398
Psi (degrees)
Phi (degrees)
Plot statistics

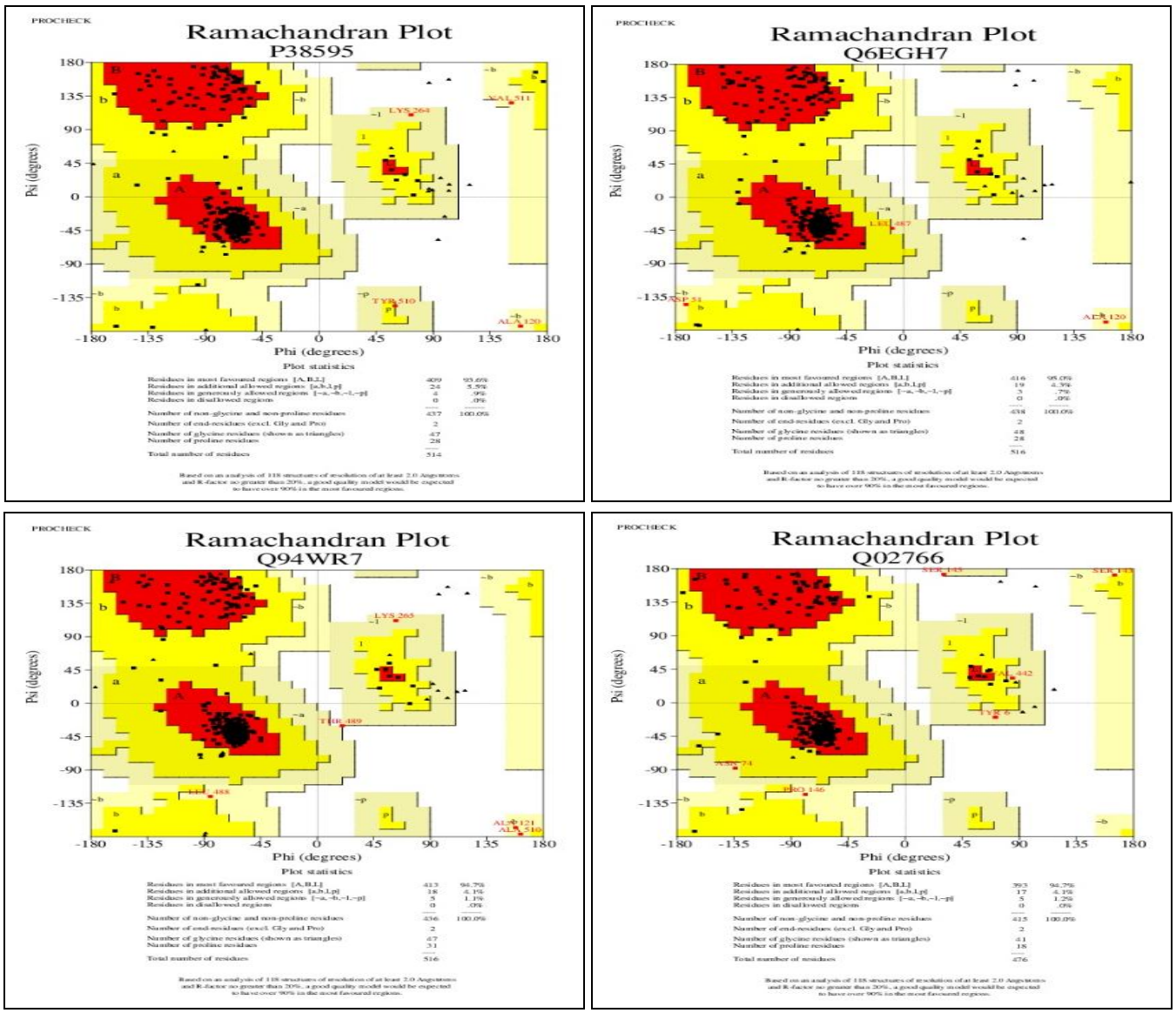

FIG. 2: RAMACHANDRAN PLOTS OF CYTOCHROME C OXIDASE SUBUNIT 1 PROTEINS FROM DIFFERENT SPECIES

TABLE 2: LIGAND BINDING POCKETS AS DETECTED BY USING SITEID MODULE OF TRIPOS SYBYL6.7 SOFTWARE

S. no.	Name of Species	Amino acids fall under receptor site
1	O21079_*Myxine glutinosa*	His151, Ala153, Gly154, Ser156, Gly160, Ala161, Phe164, Thr167, Ile168, Ile188, Leu199, Leu202, Ala203, Phe238, Glu242, Phe67, Ile75, Asn80, Val83, Met92, Asn98, Ser101, Leu105
2	O21399_*Struthio camelus*	Asn136, Val144, Ala147, Ile148, Leu207, Leu210, Tyr232, Thr60, Phe64, Phe68, Ser116, Ser117, Ala123, Thr125, Thr128, Val129
3	O79876_*Sus scrofa*	Gly239, Glu242, Val243, Leu246, His291, Thr31, Ser34, Tyr371, Val374, Ile37, Leu381, Arg38, Val421, Thr424, Phe425, Arg438, Arg439, Ser458, Tyr54, Asn55, Ile57, Val58, Thr59, His61, Ala62, Met65, Ile66, Val70, Gly123, Gly125, Trp126
4	P00395_*Homo sapiens*	Trp236, Gly239, Glu242, Val243, Leu246, His291, Thr31, Ser34, Tyr371, Ile37, Val374, Phe377, Leu381, Val386, Met390, Leu41, Met417, Thr424, Phe425, Gln428, Arg438, Arg439, Tyr54, Ile57, Val58, His61, Ala62, Met65, Ile66, Val70, Trp126
5	P00398_*Xenopus laevis*	Phe184, His240, Val243, Tyr244, Leu246, Ile247, Leu248, Pro249, Phe251, Met277, Ile280, His290, His291, Thr309, Ile312, Thr316, Val320, Phe344, Ile345, Phe348, Gly352, Gly355, Leu358, Ala359, Asp364, His368, Val373, His376, Val380, Leu381, Ala385, Val70, Met74, Phe78
6	P38595_*Halichoerus grypus*	Tyr261, Pro336, Met390, Phe393, Val394, His395, Pro398, Leu399, Tyr403, Leu405, Ala410, His413, Leu467, Met468, Met471, Glu481, Ala484, Trp494, Cys498.
7	Q6EGH7_*Zygogeomys trichopus*	Thr17, Met20, Trp340, Met390, Phe393, Val394, His395, Phe397, Leu399, Phe400, Leu405, Ala410, His413, Met468, Met471, Ile472, Ser484, Trp494, His496, Cys498
8	Q94WR7_*Buteo buteo*	Gly135, Asn136, Val144, Ala147, Ile148, Leu151, Ile207, Leu210, Ala27, Val30, Thr60, Ala61, Val65, Met66, Phe69, Phe110, Leu113, Leu114, Ser116, Ser117, Ala123, Val129
9	Q02766_*Plasmodium falciparum*	Gly126, Gly127, Leu133, Pro146, Val147, Ile152, Gly155, Leu156, Leu208, Gly211, Val212, Tyr237, Leu240, Phe241, Tyr31, Met61, Ile62, Ile65, Ile68, Ile69, Phe72, Phe73, Phe114, Val117, Thr121

TABLE 3: BINDING ENERGY AND PROTEIN LIGAND INTERACTIONS OF NATURAL COMPOUNDS AGAINST MODELLED O21079_*MYXINE GLUTINOSA* PROTEIN

S. no.	Ligand	Interactions	Binding Energy ΔG (Kcal/Mol)	Disassociation Constant (µM)
1	Artocarpin	Asn170 (2)	-4.95	234.15
2	Avenanthramide A	Phe505, Lys172 (2)	-6.17	300.0
3	Avenanthramide B	Asn170, Met176, Lys172	-5.56	83.90
4	Cycloartocarpin A	Asn170	-5.99	40.95
5	Cyclokievitone	Met178	-6.26	25.92
6	Eriosemaone A	Gly88, Lys172	-5.94	44.43
7	Khonklonginol A	Met171, Thr173	-5.77	58.69
8	Khonklonginol F	-	-5.98	41.33
9	Khonklonginol H	Asn170	-5.86	51.00
10	Racemosol	Lys172	-5.85	51.91
11	Celecoxib*	Gly88, Met171	-5.94	44.51
12	Valdecoxib*	Lys172	-5.80	56.52
13	Rofecoxib*	Gly88, Met 171	-6.45	18.58

TABLE 4: BINDING ENERGY AND PROTEIN LIGAND INTERACTIONS OF NATURAL COMPOUNDS AGAINST MODELLED O21399_*STRUTHIO CAMELUS* PROTEIN

S. no.	Ligand	Interactions	Binding Energy ΔG (Kcal/Mol)	Disassociation Constant (µM)
1	Artocarpin	Trp127, Arg439	-9.24	160.86 µM
2	Avenanthramide A	Trp127, His369, His291, Arg439	-8.08	1.20 µM
3	Avenanthramide B	Trp127, Arg439	-7.52	3.06 µM
4	Cycloartocarpin A	Trp127, Arg439	-10.49	20.40 nm
5	Cyclokievitone	Arg439, His369	-7.83	1.83 µM
6	Eriosemaone A	Trp127, His292, Arg439	-9.92	53.15 nm
7	Khonklonginol A	Arg439	-9.27	161.59 nm
8	Khonklonginol F	Trp127	-10.80	12.00 nm
9	Khonklonginol H	Trp127, His292	-9.44	120.29 nm
10	Racemosol	Trp127, His292	-9.22	175.01 nm
11	Celecoxib*	-	-8.26	885.50 nM
12	Valdecoxib*	Arg439	-8.35	752.19 nM
13	Rofecoxib*	Trp127, Arg439, Asp365, His291	-9.51	106.40 nM

TABLE 5: BINDING ENERGY AND PROTEIN LIGAND INTERACTIONS OF NATURAL COMPOUNDS AGAINST MODELLED O79876_*SUS SCROFA* PROTEIN

S. no.	Ligand	Interactions	Binding Energy ΔG (Kcal/Mol)	Disassociation Constant (µM)
1	Artocarpin	Tyr54, Arg439	-9.53	103.93 nM
2	Avenanthramide A	Tyr371, Arg438, Arg439, Trp126, Glu242	-7.62	2.61 µM
3	Avenanthramide B	Arg38, Arg439	-6.31	23.56 µM
4	Cycloartocarpin A	-	-8.23	924.96 nM
5	Cyclokievitone	His378, Arg38	-7.78	1.97 µM
6	Eriosemaone A	His61, His378, Glu242	-9.04	263.63 nM
7	Khonklonginol A	Tyr371	-9.19	182.46 nM
8	Khonklonginol F	Tyr371	-8.95	277.22 nM
9	Khonklonginol H	Arg438	-9.47	114.98 nM
10	Racemosol	Arg439, Tyr371	-9.32	148.25 nM
11	Celecoxib*	Gln428	-6.84	9.63 µM
12	Valdecoxib*	Arg438, Ala62	-7.91	1.6 µM
13	Rofecoxib*	Arg38, Arg439	-8.40	700.42 nM

TABLE 6: BINDING ENERGY AND PROTEIN LIGAND INTERACTIONS OF NATURAL COMPOUNDS AGAINST MODELLED P00395_*HOMO SAPIENS* PROTEIN

S. no.	Ligand	Interactions	Binding Energy ΔG (Kcal/Mol)	Disassociation Constant (µM)
1	Artocarpin	Tyr126, His368	-6.96	7.85 µM
2	Avenanthramide A	Gly355	-9.71	76.58 nM
3	Avenanthramide B	Tyr126, His291, Arg438	-5.85	51.4 µM
4	Cycloartocarpin A	Gly355	-10.27	29.61 nM
5	Cyclokievitone	Asp364, His368	-8.68	431.36 nM
6	Eriosemaone A	His368, Gly355	-9.65	84.33 nM
7	Khonklonginol A	Asp364, Ala359	-9.99	47.26 nM
8	Khonklonginol F	His376	-9.99	47.81 nM
9	Khonklonginol H	His368, Asp 364	-10.09	39.96 nM

10	Racemosol	His368, Asp364	-9.67	81.62 nM
11	Celecoxib*	His368, His290, Asp364	-8.94	277.51nM
12	Valdecoxib*	His240, His291, Thr316	-8.65	453.7nM
13	Rofecoxib*	His368, His 376, Asp 364, His290	-9.33	145.94nM

TABLE 7: BINDING ENERGY AND PROTEIN LIGAND INTERACTIONS OF NATURAL COMPOUNDS AGAINST MODELLED P00398_*XENOPUS LAEVIS* PROTEIN

S. no.	Ligand	Interactions	Binding Energy ΔG (Kcal/Mol)	Disassociation Constant (µM)
1	Artocarpin	Gly355	-8.82	341.34 nM
2	Avenanthramide A	Asp364, Thr316, Gly355	-8.25	896.97 nM
3	Avenanthramide B	-	-5.64	72.95 µM
4	Cycloartocarpin A	His376, Gly355	-10.72	13.82 nM
5	Cyclokievitone	His240, His290, His368, Leu358	-9.02	243.68 nM
6	Eriosemaone A	His368, Asp364	-9.31	150.29 nM
7	Khonklonginol A	-	-9.09	217.61 nM
8	Khonklonginol F	-	-9.56	98.23 nM
9	Khonklonginol H	-	-9.24	168.06 nM
10	Racemosol	His376	-9.14	199.08 nM
11	Celecoxib*	-	-8.23	930.24 nM
12	Valdecoxib*	His240, His290	-8.11	1.14 µM
13	Rofecoxib*	His368, Asp364	-9.21	177.51 nM

TABLE 8: BINDING ENERGY AND PROTEIN LIGAND INTERACTIONS OF NATURAL COMPOUNDS AGAINST MODELLED P38595_*HALICHOERUS GRYPUS* PROTEIN

S. no.	Ligand	Interactions	Binding Energy ΔG (Kcal/Mol)	Disassociation Constant (µM)
1	Artocarpin	Lys13, Phe400, Tyr502	-6.90	8.81 µM
2	Avenanthramide A	Thr17, Thr502, Thr17	-7.55	2.91 µM
3	Avenanthramide B	Lys13, Phe400, Tyr17	-6.33	22.9 µM
4	Cycloartocarpin A	Lys13	-9.04	236.84 nM
5	Cyclokievitone	Lys13, Pro500, Ser401	-7.92	1.55 µM
6	Eriosemaone A	Thr17	-8.34	771.67 nM
7	Khonklonginol A	Lys13, Thr17, Pro500	-8.35	762.44 nM
8	Khonklonginol F	Lys13, Pro500	-8.12	1.12 µM
9	Khonklonginol H	Ser401	-7.85	1.77 µM
10	Racemosol	Ser401, Pro500	-8.91	292.46 nM
11	Celecoxib*	Lys13	-7.98	1.14 µM
12	Valdecoxib*	Lys13, ASP14	-8.26	877.06nM
13	Rofecoxib*	Lys13	-8.58	650.82nM

TABLE 9: BINDING ENERGY AND PROTEIN LIGAND INTERACTIONS OF NATURAL COMPOUNDS AGAINST MODELLED Q6EGH7_*ZYGOGEOMYS TRICHOPUS* PROTEIN

S. no.	Ligand	Interactions	Binding Energy ΔG (Kcal/Mol)	Disassociation Constant (µM)
1	Artocarpin	Arg5, Lys13, Asp14	-9.78	67.63 nM
2	Avenanthramide A	Lys13, Pro500, Asp14	-8.03	1.29 µM
3	Avenanthramide B	Lys13, Thr401	-8.04	1.28 µM
4	Cycloartocarpin A	-	-6.66	13.21 µM
5	Cyclokievitone	Lys13	-8.15	1.07 µM
6	Eriosemaone A	Arg5	-8.17	1.03 µM
7	Khonklonginol A	Arg5, Asp14, Pro500	-8.59	504.7 nM
8	Khonklonginol F	Arg480, Thr401	-9.10	213.32 nM
9	Khonklonginol H	-	-9.13	204.0 nM
10	Racemosol	Thr401	-8.74	392.28 nM
11	Celecoxib*	Lys13	-8.08	1.19 µM
12	Valdecoxib*	Lys13, Pro500	-8.60	500.75Nm
13	Rofecoxib*	Asn11, Lys13, Asp14	-8.41	650.82nM

TABLE 10: BINDING ENERGY AND PROTEIN LIGAND INTERACTIONS OF NATURAL COMPOUNDS AGAINST MODELLED Q94WR7_*BUTEO BUTEO* PROTEIN

S. no.	Ligand	Interactions	Binding Energy ΔG (Kcal/Mol)	Disassociation Constant (µM)
1	Artocarpin	Ala123, Ser143	-6.83	9.43 µM
2	Avenanthramide A	Ala123, Ser143	-7.72	2.19 µM
3	Avenanthramide B	-	-5.68	68.95 µM
4	Cycloartocarpin A	Val119	-6.96	7.88 µM
5	Cyclokievitone	Ser117	-7.47	3.35 µM

6	Eriosemaone A	Leu113	-7.21	5.21 µM
7	Khonklonginol A	-	-7.43	3.59 µM
8	Khonklonginol F	Ala123	-7.47	3.37 µM
9	Khonklonginol H	-	-6.85	9.47 µM
10	Racemosol	Ala123	-7.05	6.80 µM
11	Celecoxib*	-	-7.46	3.43 µM
12	Valdecoxib*	-	-7.72	2.17 µM
13	Rofecoxib*	Ala123	-8.94	279.83nM

TABLE 11: BINDING ENERGY AND PROTEIN LIGAND INTERACTIONS OF NATURAL COMPOUNDS AGAINST MODELLED Q02766_*PLASMODIUM FALCIPARUM* PROTEIN

S. no.	Ligand	Interactions	Binding Energy ΔG (Kcal/Mol)	Disassociation Constant (µM)
1	Artocarpin	-	-4.52	488.63 µM
2	Avenanthramide A	-	-4.01	1.16 µM
3	Avenanthramide B	Thr209	-3.43	3.08 mM
4	Cycloartocarpin A	-	-5.21	152.82 µM
5	Cyclokievitone	Phe154	-4.68	371.81 µM
6	Eriosemaone A	-	-5.33	124.09 µM
7	Khonklonginol A	-	-5.22	148.48 µM
8	Khonklonginol F	-	-5.15	167.27 µM
9	Khonklonginol H	-	-5.18	159.22 µM
10	Racemosol	-	-5.29	132.15 µM
11	Celecoxib*	-	-6.64	13.48 µM
12	Valdecoxib*	Thr209	-4.99	221.22 µM
13	Rofecoxib*	Thr209	-5.32	126.61 µM

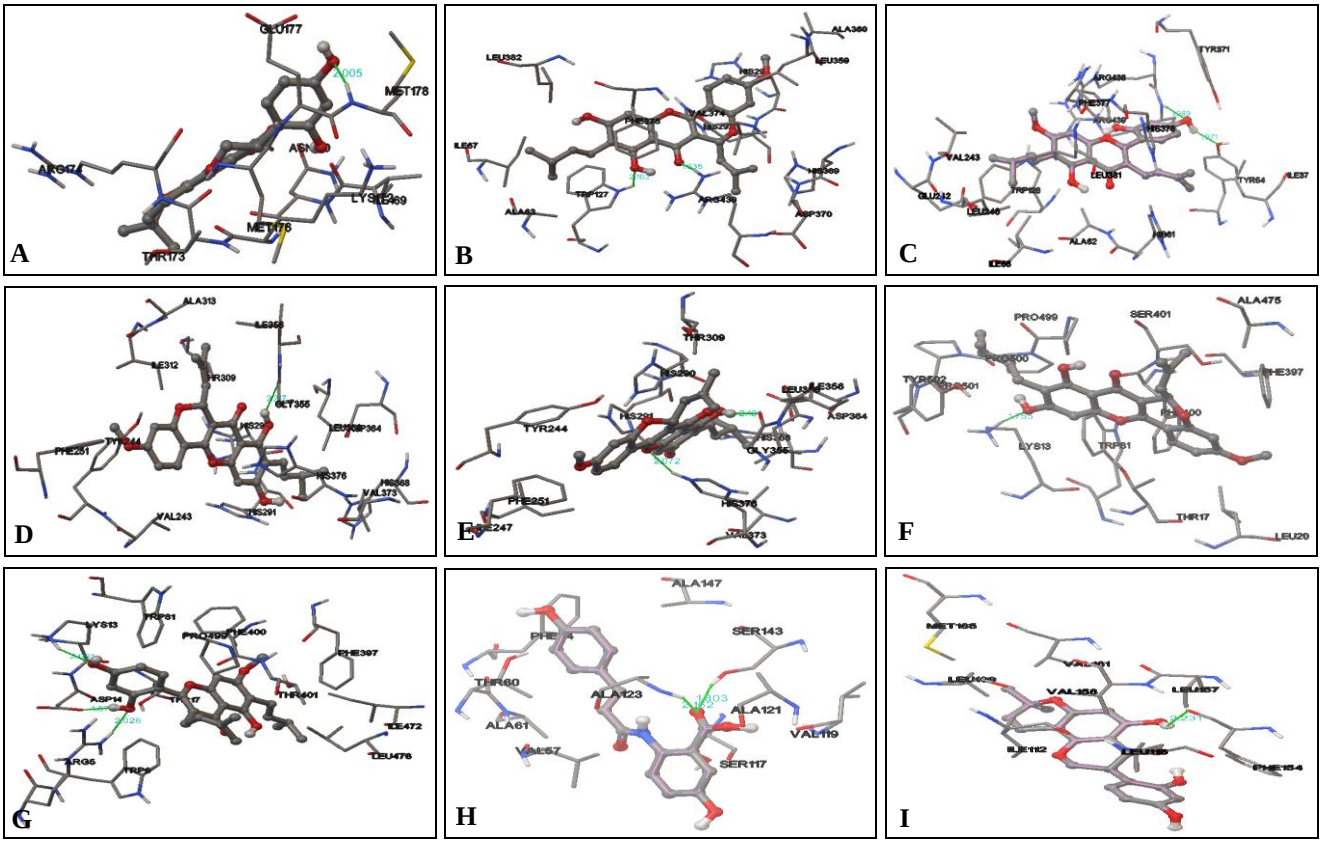

FIG. 3: INTERACTIONS OF CYCLOKIEVITONE INTERACTIONS WITH CYTOCHROME C OXIDASE SUBUNIT 1 FROM *MYXINE GLUTINOSA* [B] CYCLOARTOCARPIN A INTERACTIONS WITH CYTOCHROME C OXIDASE SUBUNIT 1 FROM *STRUTHIO CAMELUS* [C] ARTOCARPIN INTERACTIONS WITH CYTOCHROME C OXIDASE SUBUNIT 1 FROM *SUS SCROFA*,[D] CYCLOARTOCARPIN A INTERACTIONS WITH CYTOCHROME C OXIDASE SUBUNIT 1 FROM *HOMO SAPIENS* [E] CYCLOARTOCARPIN A INTERACTIONS WITH CYTOCHROME C OXIDASE SUBUNIT 1 FROM *XENOPUS LAEVIS*, [F] CYCLOARTOCARPIN A INTERACTIONS WITH CYTOCHROME C OXIDASE SUBUNIT 1 FROM *HALICHOERUS GRYPUS*, [G] ARTOCARPIN INTERACTIONS WITH CYTOCHROME C OXIDASE SUBUNIT 1 FROM *ZYGOGEOMYS TRICHOPUS*, [H] AVENANTHRAMIDE A INTERACTIONS WITH CYTOCHROME C OXIDASE SUBUNIT 1 FROM *BUTEO BUTEO*, *[I]* RACEMOSOL INTERACTIONS WITH CYTOCHROME C OXIDASE SUBUNIT 1 FROM *PLASMODIUM FALCIPARUM*

CONCLUSION: In the present study, the stable three-dimensional models were constructed for Cytochrome c oxidase protein from nine different species and further used for molecular docking with the natural inhibitors. Molecular docking results revealed some important amino-acid residues in the active sites of Cytochrome c oxidase protein, which play a key role in the maintenance of their conformation and are directly associated with substrate binding. The interactions between the ligands and the binding sites of Cytochrome c oxidase protein shown in the present study are useful for the understanding of the binding mechanisms of inhibitors and active site information of these proteins. The use of combinatorial approaches may result in the rapid development of better anti-inflammatory and anti-proliferative in future. Successful docking methods search high-dimensional spaces effectively and use a scoring function that correctly ranks candidate dockings. Molecular docking studies of the above compounds showed favorable interactions in the binding site of the modeled COX proteins. Therefore, it is concluded that these molecules are the potential candidates for cytochrome c oxidase inhibitors.

ACKNOWLEDGEMENT: Nil

CONFLICTS OF INTEREST: None

REFERENCES:

1. Capaldi RA: Structure and function of cytochrome c oxidase. Annu Rev Biochem 1990; 59: 569-96.
2. Michaela C, Struder K and Denis HL: Comparative analysis of the mitochondrial cytochrome c oxidase subunit I (COI) gene in ciliates (Alveolata, Ciliophora) and evaluation of its suitability as a biodiversity marker 2010; 8(1): 131-48.
3. Heller P, Casaletto J, Ruiz G and Jonathan G: Data Descriptor: A database of metazoan cytochrome c oxidase subunit I gene sequences derived from GenBank with CO-ARBitrator. Scientific Data 2018; 5: 180156.
4. Rodrigues MS, Morelli KA and Jansen AM: Cytochrome c oxidase subunit 1 gene as a DNA barcode for discriminating Trypanosoma cruzi DTUs and closely related species. Parasit Vectors 2017; 10: 488.
5. Michel H, Behr J, Harrenga A and Kannt A: Cytochrome c oxidase: structure and spectroscopy. Annu Rev Biophys Biomol Struct 1998; 27: 329-56.
6. Denis M: Structure and function of cytochrome-c oxidase. Biochimie 1986; 68(3): 459-70.
7. Cooper CE, Nicholls P and Freedman JA: Cytochrome c oxidase: structure, function, and membrane topology of the polypeptide subunits. Bioch Cell Biol 1991; 69(9): 586-07.
8. Wikstrom M, Saraste M and Penttila T: Relationships between structure and function in cytochrome oxidase. In AN Martonosi, ed, The Enzymes of Biological Membranes, 4. Plenum, New York 1985; 111-48.
9. Fox TD and Leaver CJ: The *Zea mays* mitochondrial gene coding cytochrome oxidase subunit II has an intervening sequence and does not contain TGA codons. Cell 1981; 26(3 Pt 1): 315-23.
10. Hiesel R, Schobel W, Schuster W and Brennicke A: The cytochrome oxidase subunit I and subunit III genes in Oenothera mitochondria are transcribed from identical promoter sequences. EMBO J 1987; 6(1): 29-34.
11. Isaac PG, Jones VP and Leaver CJ: The maize cytochrome c oxidase subunit I gene: sequence, expression and rearrangement in cytoplasmic male sterile plants. EMBO J 1985; 4(7): 1617-23.
12. McCarty DM, Hehman GL and Hauswirth WW: Nucleotide sequence of the *Zea mays* mitochondrial cytochrome oxidase subunit III gene. Nucleic Acids Res 1988; 16(20): 9873.
13. UniProt Consortium. UniProt: a worldwide hub of protein knowledge. Nucleic Acids Res 2019; 47(D1): D506-D515.
14. Camacho C, Coulouris G, Avagyan V, Ma N, Papadopoulos J, Bealer K and Madden TL: BLAST+: architecture and applications. BMC Bioinformatics 2009; 10: 421.
15. Larkin MA, Blackshields G, Brown NP, Chenna R, McGettigan PA, McWilliam H, Valentin F, Wallace IM, Wilm A, Lopez R, Thompson JD, Gibson TJ, Higgins DG, Clustal W and Clustal X: version 2.0. Bioinformatics, 2007; 23(21): 2947-48,
16. Webb B and Sali A: Comparative Protein Structure Modeling Using Modeller. Current Protocols in Bioinformatics 54, John Wiley & Sons, Inc 2016; 5.6.1-5.6.37.
17. Eswar N, Webb B, Marti-Renom MA, Madhusudhan MS, Eramian D, Shen MY, Pieper U and Sali A: Comparative protein structure modeling using modeller. Curr Protoc Bioinformatics 2006; 0 5: Unit-5.6.
18. Bitencourt-Ferreira G and Filgueira de Azevedo Jr W: Homology modeling of protein targets with MODELLER. Methods Mol Biol 2019; 2053: 231-249.
19. Laskowski RA, MacArthur MW, Moss DS and Thornton JM: PROCHECK - a program to check the stereochemical quality of protein structures. J App Crys 1993; 26: 283-91.
20. Sybyl 6.7, Tripos Associates, 1699 South Hanley Road, St. Louis, USA, MO 63144.
21. Veeraswamy B, Madhu D, Dev GJ, Poornachandra Y, Kumar GS, Kumar CG and Narsaiah B: Studies on synthesis of novel pyrido[2,3-d]pyrimidine derivatives, evaluation of their antimicrobial activity and molecular docking. Bioorg Med Chem Lett 2018; 28(9): 1670-75.
22. Banu S, Bollu R, Nagarapu L, Nanubolu JB, Yogeswari P, Sriram D, Gunda SK and Vardhan D: Design, synthesis, and *in-vitro* antitubercular activity of 1,2,3-triazolyl-dihydroquinoline derivatives. Chem Biol Drug Des 2018; 92(1): 1315-23.

How to cite this article:
Mallojala V, Pasam K, Gunda SK, Bandi S and Shaik M: Comparative modelling and docking studies of cytochrome c oxidase subunit 1 protein. Int J Pharm Sci & Res 2020; 11(10): 5148-57. doi: 10.13040/IJPSR.0975-8232.11(10).5148-57.